

Soft Matter

Accepted Manuscript



This is an *Accepted Manuscript*, which has been through the Royal Society of Chemistry peer review process and has been accepted for publication.

Accepted Manuscripts are published online shortly after acceptance, before technical editing, formatting and proof reading. Using this free service, authors can make their results available to the community, in citable form, before we publish the edited article. We will replace this *Accepted Manuscript* with the edited and formatted *Advance Article* as soon as it is available.

You can find more information about *Accepted Manuscripts* in the [Information for Authors](#).

Please note that technical editing may introduce minor changes to the text and/or graphics, which may alter content. The journal's standard [Terms & Conditions](#) and the [Ethical guidelines](#) still apply. In no event shall the Royal Society of Chemistry be held responsible for any errors or omissions in this *Accepted Manuscript* or any consequences arising from the use of any information it contains.



Journal Name

ARTICLE

Investigation of splashing phenomena during the impact of molten sub-micron gold droplets on solid surfaces

Daozhi Shen,^a Guisheng Zou,^{a,b} Lei Liu,^{*a,b} Walter W. Duley^{c,d} and Y. Norman Zhou^{a,c,e}

Received 00th January 20xx,
Accepted 00th January 20xx

DOI: 10.1039/x0xx00000x

www.rsc.org/

The dynamics of splashing accompanying the impact of molten 800 nm diameter gold droplets on silicon, gold coated silicon, gold coated glass and polished solid gold surfaces has been studied. A novel method based on laser induced forward transfer has been developed to generate single submicron molten gold droplets. Splashing morphology has been characterized using Scanning Electron Microscopy (SEM) and Focused Ion Beam (FIB) techniques. It is found that the splashing of submicron gold droplets on impact is enhanced by high droplet impact energy achieved by reducing the droplet flight distance and that an air layer resulting in a bubble becomes trapped under the impacting droplet even when the size of the droplet is less than one micron. Our results show that, under these conditions, heat transfer between the submicron droplet and the solid substrate is more important than surface roughness and surface tension in the evolution of splashing. A theoretical model has been developed to simulate the splashing characteristics of submicron gold droplets during impact. Both the experimental data and the analytical model show that splashing is enhanced by high heat transfer rates to the surface.

Introduction

Splashing of a high-speed droplet on hitting a dry solid surface is ubiquitous in nature and is an important phenomenon in many technological and scientific processes. The impingement of molten droplets on surfaces plays a crucial role in many industrial applications including suspension plasma-sprayed coating¹, micron additive fabrication² and laser induced transfer (LIT)³⁻⁵. For example, deposition of submicron gold droplets on substrate can be applied for additive fabrication, which requires gold material as receiver to improve the adhesion of droplets⁶. Besides, using laser induced forward transfer (LIFT) technique to deposit gold nanodroplets on silicon substrate in micron period arrays allows optoelectronics applications⁷. Until now, most studies about LIFT technique have focused on extending the range of materials⁸⁻¹¹ that able to be deposited using LIFT and focused on fabricating plasmonic devices by LIFT^{5, 12-14}. However, it has been rarely reported about investigation on the shape of particles deposited on substrate, which is important for application of LIFT.

The splashing of droplets at room temperature is a result of many interacting physical effects. These include surface roughness,^{15, 16} the inertia of the droplet,¹⁷ the contact angle^{18, 19}

and air pressure^{20, 21}. Splashing of high temperature molten droplets on hitting a cold solid substrate is also influenced by the substrate temperature and heat transfer between the molten droplet and the substrate²², making the physical process even more complex. The focus in most of these studies has been in characterizing the impact dynamics of droplets with sizes > 10 μm. Until now, little work has been carried out on the impact dynamics of molten submicron droplets primarily because of difficulties in generating single high-speed submicron molten droplets in a controllable way followed by direct observation of the impact process²³. As a result, we currently have little knowledge on the processes associated with the impact of molten submicron droplets on dry solid substrates²³.

In this paper, we use a femtosecond laser induced forward transfer (fsLIFT) technique to generate individual high-speed submicron gold droplets and study the impact of these droplets on a variety of solid substrates. Observation of the morphology of solidified droplets after they have spread following impact on substrate reveals the mechanisms involved in splashing. In this work we report a study of the splashing of molten submicron gold droplets on substrates with different thermal properties and investigate the role of heat transfer during impact on the evolution of splashing. A theoretical model is also developed to enhance understanding of this process.

Experiment procedure

In these experiments, we used a commercial femtosecond laser system (Coherent) delivering laser pulses at a central wavelength of 800 nm, with a maximum pulse energy of 4 mJ, and a pulse duration of 50 fs at the maximum repetition rate of 1 kHz. A 60 nm

^a Department of Mechanical Engineering, Tsinghua University, Beijing, 100084, China. E-mail: liulei@tsinghua.edu.cn

^b The State Key Laboratory of Tribology, Tsinghua University, Beijing, 100084, China.

^c Centre for Advanced Materials Joining, University of Waterloo, Waterloo, Ontario N2L 3G1, Canada

^d Department of Physics and Astronomy, University of Waterloo, Waterloo, Ontario N2L 3G1, Canada

^e Department of Mechanical & Mechatronics Engineering, University of Waterloo, Waterloo, N2L 3G1 Canada.

gold film donor layer, coated on a 320 μm thick glass substrate, was fabricated by magnetron sputtering and was used for laser transfer of molten submicron gold droplets. To obtain submicron gold droplets having a diameter of ~ 800 nm, single fs laser pulses with an energy of ~ 0.7 μJ were focused by a microscope objective (Olympus) with $\times 10$ magnification and a numerical aperture (NA) of 0.3 through the glass onto the thin gold donor film (see Fig. 1a). The substrate that received the droplets was placed close to the gold coated glass at distances of < 10 μm , 60 μm and 120 μm . The donor substrate and receiver substrate were placed on an XYZ stage and moved horizontally at a velocity of 0.2 mm/s. The femtosecond laser pulse repetition rate was set 20 Hz to ensure that individual pulses irradiated a fresh gold area as shown in Fig. 1a. In Fig. 1b we show a detailed schematic of the experimental set-up. A neutral density (ND) filter and a $\lambda/2$ plate, together with a polarizer, were set up to continuously attenuate the incident laser radiation. The laser and light from a halogen lamp entering the objective are coaxial, so a CCD camera can be used to check whether the interface between the gold film and the glass is at the focal plane of the objective. All processing was carried out in air at atmospheric pressure.

Imaging with a high speed camera is traditionally used to capture side or bottom views of the droplet as it spreads or splashes during impact^{3, 16, 24-26}. However, it is difficult to obtain clear images of submicron size, high velocity droplets using this technique. Instead, we use SEM (TESCAN Inc.) images of solidified submicron gold droplets after deposit to see whether splashing occurs after hitting the dry solid surface. Details of structure inside the solidified droplets were analysed by cross-sectioning the solidified gold droplets by FIB (TESCAN Inc.). Fabrication procedures involved in obtaining metal cross-sections are shown in Fig. 2. A platinum coating was deposited prior to FIB milling to protect the gold surface upon exposure to the Ga⁺ beam. FIB milling of the deposited gold proceeded vertically as shown in Fig. 2.

In order to investigate how heat transfer rate between droplet and substrate affects splashing result, four different types of substrates were used as the receptors for transferred metal: (1) single crystal silicon with a thickness of 500 μm and an average surface roughness of 0.4 nm; (2) a 60 nm gold film coated on a 300 μm thick glass and an average surface roughness of 1.2 nm; (3) a 50 nm gold film coating on a silicon wafer with a 5 nm chromium adhesion layer and an average surface roughness of 4.1 nm (PELCO); (4) a polished gold foil with a thickness of 30 μm and an average surface roughness of 6.0 nm.

The same laser parameters and donor substrate were used in each experiment in order to reproduce the droplet size, the initial speed and temperature of droplets ejected from the gold film. Experimental conditions were maintained for deposition of at least 20 individual droplets, but high magnification images will be shown for only one of these droplets.

Result

Fig. 3a shows the morphology of a periodic array of solidified metal particles deposited using the fsLIFT technique after impact and spreading on the surface of a 50 nm thick gold film coating on silicon at a droplet flight distance of 60 μm . A magnified view of one

transferred gold particle is shown in Fig. 3b. Splashing morphologies of each of the metal deposits were almost same, forming symmetric crown-like splashes, indicating that uniform splashing behavior can be obtained when the irradiation conditions are standardized. The particles deposited on the surface of polished gold foil are shown in Fig. 3c, with a magnified view shown in Fig. 3d. In this condition, the metal deposits were all spherical with diameter of ~ 800 nm, indicating the droplet size in all deposition conditions.

As noted elsewhere, the velocity of molten submicron droplets ejected from a gold film after irradiation by a femtosecond laser pulse is tens of meters per second²⁷. Due to the drag force in air and convective cooling, the velocity and temperature of such droplets will decrease prior to impact on the receptor substrate. Neglecting quantum effects and the Brownian motion of droplets during flight, the drag force, f , acting on these droplets in air is

$$f = -kR^3v \quad (1)$$

where k is a constant, R is the diameter of the droplet and v is the relative velocity of the droplet in air.^{28, 29} From Newton's law

$$v = v_0 - \frac{kR^3z}{m} \quad (2)$$

$$t_f = \frac{m}{kR^3} \ln \frac{v_0}{v} \quad (3)$$

where v_0 is the initial velocity of the droplet ejected from the gold film on the donor substrate, m is the mass of the droplet, z is the flight distance and t_f is time measured from the ejection of the droplet.

The reduction in droplet temperature prior to impact due to heat transfer to the ambient air is³⁰

$$T_d = T_{room} + (T_{eject} - T_{room}) \exp\left(-\frac{a\epsilon t_f}{R\lambda}\right) \quad (4)$$

where $T_d(t)$ is the temperature of the droplet during flight, T_{room} is room temperature, T_{eject} is the temperature of the droplet ejected from the donor substrate, ϵ is the heat transfer coefficient between the droplet and the surrounding air, λ is the thermal conductivity coefficient of the droplet material and $a = \lambda/\rho c$ where ρ is the density of the droplet and c is its specific heat capacity. Considering momentum and kinetic energy, the total energy of the droplet before impacting the substrate is

$$E = \frac{1}{2}mv^2 + \frac{3}{2}Nk_B T_d \\ = \frac{1}{2}m\left(v_0 - \frac{kR^3z}{m}\right)^2 + \frac{3}{2}Nk_B [T_{room} + (T_{eject} - T_{room})\left(1 - \frac{kR^3z}{mv_0}\right)^{\frac{\epsilon am}{k\lambda R^3}}] \quad (5)$$

Here N is the number of atoms in the droplet and k_B is Boltzmann constant. Equation (5) indicates that the total energy of droplet decreases with flight distance z . Distances between the donor substrate and the receiver substrate are set at < 10 μm , 60 μm and 120 μm to achieve different values for E (droplet) before it impacts the substrate.

Fig. 4 shows the effect of different flight distances on the impact of 800 nm diameter molten gold droplets on a silicon surface. At high impact energy ($z < 10$ μm , as shown in Fig. 4a), splashing produces an irregular lamella-like morphology and a small droplet is ejected away from the lamella. No splash was visible at

smaller impact energies ($z = 60 \mu\text{m}$ and $120 \mu\text{m}$, as shown in Fig. 4b and c, respectively). In this case, the lamella did not become unstable but uniformly spread to form a thin disk-like splat structure with a thicker smooth rim at the periphery. Although droplet temperature decreases as the flight distance increases, these results indicate that the submicron gold droplet was still liquid after travelling the maximum distance of $120 \mu\text{m}$.

Fig 5 shows the morphology of gold droplets after impact on a polished gold foil, > 35 times thicker than the diameter of the gold droplet. Under these conditions, the gold foil has large mass compared to that of the droplet, and behaves like a bulk material. At high impact energy, the molten gold droplet is observed to splash on the gold substrate as shown in Fig. 5a. However, no splashing occurred at intermediate impact energy (Fig. 5b), although the periphery exhibits the effect of instabilities in the liquid surface. At low impact energy (Fig. 5c), the droplet remains spherical after impact as droplet solidification is rapid, inhibiting spreading.

The above results clearly show that heat transfer to the substrate plays an important role in determining spreading and splashing of a molten submicron droplet. Gold coated glass substrate and gold coated silicon substrates were used to obtain different heat transfer rates without changing wetting conditions. Figs. 6 and 7 show images of molten submicron droplets impacting on gold coated glass and gold coated silicon, respectively. The splashing behaviors in Fig. 6 and 7 are seen to be very similar and are not influenced by surface roughness. In both Figs. 6 and 7, asymmetric splashes with irregular edges were found at high impact energy and result from the ejection of lamella. At intermediate impact energy (Figs. 6b and 7b), symmetric splashes with crown-like outward propagating drops are observed (similar to the morphology shown in Fig. 3b), while at low impact energy (Figs. 6c and 7c), no splashing was visible and random bumps formed at the edges of the ring. These bumps can be associated with the initial stages in the development of the crown-like structures seen at higher impact energy. Observation of splashing morphology on the four substrates at different droplet flight distance shows that splashing is enhanced for submicron droplet impact on gold coated silicon and gold coated glass compared to impact on silicon. A summary of splashing behaviors of sub-micron gold droplet impacting on different substrates with different flight distances is shown in Table 1.

Cross-sections of submicron droplets after impact and sectioning using FIB are shown in Figs. 4-7. Entrapped air bubbles or air layers, as indicated by arrows, were observed at the center of the droplet-substrate interface. Air layers and bubbles entrapped between micron-sized room temperature droplets and a solid surface have been seen in previous studies and it is evident that these structures play a significant role in determining the overall structures remaining after impact^{21, 31, 32}. Direct measurement of the air layer has been obtained using optical interferometry. However, this technique is not available for submicron droplets due to diffraction. Entrapped air layers and air bubbles in our experiments are believed to be firm evidence for the existence of an air layer during impact. This is the first time that such entrapped structures have been detected after impact quenching of molten submicron droplets. Their presence indicates that, as for molten submicron droplets, the onset of deformation in these droplets

arises from a rapid pressure increase in the air layer trapped between the liquid and the solid surface during impact.

Discussion

Other studies have demonstrated that splashing is diminished for room temperature droplets when the material readily wets the surface^{18, 19}. In the current study, we find, however, that splashing is enhanced on a gold coated silicon substrate relative to a silicon substrate (Fig 4b and Fig. 7b), which is an opposite effect. We suggest that a hot droplet/cold substrate combination increases the role of heat transfer allowing heat transfer to become more important than surface wetting. The following section will discuss this heat transfer in some detail.

In a model based on splashing induced by the trapped air layer,^{17, 20, 32, 33} the droplet approaches close to substrate and initially forms an air dimple due to compression of the ambient gas between the droplet and the surface. Once the droplet touches the substrate, a viscous boundary layer develops near the contact region, as shown in Fig. 8. Viscous drag decreases the horizontal flow coming from the center of the droplet, which diverts the flow away from the surface and lifts the lamella³². Instability in the lamella during liftoff leads to the ejection of material and splashing. To describe this process, we consider two contributions to the stress on the expanding liquid layer: Σ_G due to the restraining pressure of the air layer, which acts to deflect material upward, and Σ_L due to surface tension, which keeps the liquid layer intact^{20, 32}. Thus droplet splashing results from the competition between these two forces, with Σ_G promoting splashing through sheet ejection and Σ_L suppressing this effect. As described by Xu *et al.* in ref.20, Σ_G/Σ_L is approximately

$$\Sigma_G/\Sigma_L = \sqrt{\gamma M_G} P \sqrt{\frac{R v_H \sqrt{v_L}}{2 k_B T \sigma}} \quad (6)$$

implying that splashing occurs when Σ_G/Σ_L reaches a critical value. Here P is the ambient atmospheric pressure, M_G is the molecular weight of the gas, γ is the adiabatic constant of the gas, T is the temperature, k_B is Boltzmann's constant, R is the initial radius of the drop, v_H is impact velocity, σ is the surface tension coefficient and v_L is the kinematic viscosity of the liquid.

The physical quantities in equation (6) are evaluated at room temperature and are assumed to be constant. They would vary from these values only when a temperature gradient exists between the droplet and the substrate. To simplify, we only consider heat transfer between the viscous boundary layer and the substrate. From ref.30 the temperature of the viscous boundary layer is

$$T(h, t) = T_s + (T_d - T_s) \exp\left(-\frac{h t}{l}\right) \quad (7)$$

where, T_s is the temperature of the substrate before droplet impact, T_d is the temperature of the droplet when it reaches the substrate, h is the heat transfer coefficient between the droplet and the substrate, t is time measured from the instant of impact and l is the thickness of viscous boundary layer. This result can then be used to find the droplet temperature during the impact process as a function of h and t . The surface tension coefficient $\sigma = \sigma_0(1 - T/T_0)$,

increases as temperature decreases³⁴. T_C is the critical temperature and σ_0 is an empirical coefficient. Considering equation (7) and the temperature dependence of σ ,

$$\begin{aligned}\Sigma_G/\Sigma_L &= \sqrt{\gamma M_G} P \sqrt{\frac{Rv_H}{2k_B T} \frac{\sqrt{v_L}}{\sigma}} \\ &= \sqrt{\gamma M_G} \frac{P}{\sigma_0} \sqrt{\frac{Rv_H}{2k_B} \frac{\sqrt{v_L(T(h,t))}}{\sqrt{T(h,t)-2T(h,t)^2/T_C+T(h,t)^3/T_C^2}}} \\ &= \sqrt{\gamma M_G} \frac{P}{\sigma_0} \sqrt{\frac{Rv_H}{2k_B} F(T(h,t))}\end{aligned}\quad (8)$$

As $F(T)$ is a monotonic function of T , when Σ_G/Σ_L becomes equal to a critical value droplet splashing occurs. At this critical temperature, $T = T_c$. Then the time at which $T(h,t) = T_c$, is from equation (7)

$$t = \frac{l\lambda}{ha} \ln \frac{T_d - T_s}{T_c - T_s} \quad (9)$$

Equation (9) implies that the splashing time decreases with an increase in heat transfer between the droplet and the substrate, so that the molten droplet splashes more easily when the heat transfer to the substrate increases.

Comparing the cross-sectional images of metal droplets deposited on different substrates, we see that the residual top on the impacted droplet on a gold foil (Fig. 5e) is much more pronounced than that on gold coated silicon or glass (Figs. 6e and 7e). The droplet on silicon had the smallest residual top (see Fig. 4e). The height of this residual top on the droplet is affected by the heat transfer efficiency between the droplet and the substrate. A higher residual top on the droplet implies a larger heat transfer rate to the substrate, so that less liquid can spread from the center to the edges before the center of the metal can solidify. Based on the above analytical model, it is apparent that submicron gold droplets exhibit increased splashing on gold coated silicon and gold coated glass substrates relative to silicon substrates because of the higher heat transfer rate for gold-gold contact compared to that at the gold-silicon interface. The experimental data also shows that, if heat transfer is too efficient, then the entire droplet freezes too quickly to permit significant flow/ejection of metal from the cooling droplet. Under these conditions, splashing does not occur, as shown in Fig. 5b and c.

Conclusions

We have developed a new technique based on femtosecond laser induced forward transfer (fsLIFT) and focused ion beam (FIB) milling to investigate the splashing behavior of molten submicron droplets. This new method has shown that an air layer and/or air bubbles become entrapped underneath submicron sized droplets during impact. From a comparison of splashing characteristics under standardized conditions on different substrates, we find that heat transfer between the molten submicron droplet and the solid substrate is the primary factor controlling the evolution of splashing morphology. Splashing is enhanced at higher impact energy, but average surface roughness ≤ 6 nm and the wettability of the substrate surface are not as important as heat transfer to the substrate on a submicron scale. These experiments, supported by

an analytical model, show that higher droplet-substrate heat transfer rates facilitate splashing.

Acknowledgements

This work was supported by National Natural Science Foundation of China (Grant No. 51375261, 51405258, 51520105007), by The Natural Science Foundation of Beijing (Grant No. 3132020), by The Specialized Research Fund for Doctoral Program of Higher Education (Grant No. 20130002110009) and by Tsinghua University Initiative Scientific Research Program (Grant No. 2010THZ 02-1 2013Z02-1).

References

1. K. VanEvery, M. M. Krane, R. Trice, H. Wang, W. Porter, M. Besser, D. Sordelet, J. Ilavsky and J. Almer, *J Therm Spray Tech*, 2011, **20**, 817-828.
2. M. Vaezi, H. Seitz and S. Yang, *Int J Adv Manuf Technol*, 2013, **67**, 1721-1754.
3. U. Zywiets, A. B. Evlyukhin, C. Reinhardt and B. N. Chichkov, *Nat Commun*, 2014, **5**, 3402.
4. L. Yang, C.-y. Wang, X.-c. Ni, Z.-j. Wang, W. Jia and L. Chai, *Applied Physics Letters*, 2006, **89**, 161110.
5. A. I. Kuznetsov, A. B. Evlyukhin, M. R. Gonçalves, C. Reinhardt, A. Koroleva, M. L. Arnedillo, R. Kiyon, O. Marti and B. N. Chichkov, *Acs Nano*, 2011, **5**, 4843-4849.
6. A. Kuznetsov, R. Kiyon and B. Chichkov, *Opt. Express*, 2010, **18**, 21198-21203.
7. D. P. Banks, C. Grivas, J. D. Mills, R. W. Eason and I. Zergioti, *Applied Physics Letters*, 2006, **89**, 193107.
8. P. Papakonstantinou, N. Vainos and C. Fotakis, *Applied surface science*, 1999, **151**, 159-170.
9. S. Bera, A. Sabbah, J. Yarbrough, C. Allen, B. Winters, C. G. Durfee and J. A. Squier, *Applied optics*, 2007, **46**, 4650-4659.
10. A. Narazaki, T. Sato, R. Kurosaki, Y. Kawaguchi and H. Niino, *Applied Physics Express*, 2008, **1**, 057001.
11. L. Koch, A. Deiwick, S. Schlie, S. Michael, M. Gruene, V. Coger, D. Zychlinski, A. Schambach, K. Reimers, P. M. Vogt and B. Chichkov, *Biotechnol Bioeng*, 2012, **109**, 1855-1863.
12. M. L. Tseng, Y.-W. Huang, M.-K. Hsiao, H. W. Huang, H. M. Chen, Y. L. Chen, C. H. Chu, N.-N. Chu, Y. J. He and C. M. Chang, *ACS nano*, 2012, **6**, 5190-5197.
13. W. T. Chen, M. L. Tseng, C. Y. Liao, P. C. Wu, S. Sun, Y.-W. Huang, C. M. Chang, C. H. Lu, L. Zhou and D.-W. Huang, *Opt. Express*, 2013, **21**, 618-625.
14. M. L. Tseng, C. M. Chang, B. H. Chen, Y. W. Huang, C. H. Chu, K. S. Chung, Y. J. Liu, H. G. Tsai, N. N. Chu, D. W. Huang, H. P. Chiang and D. P. Tsai, *Nanotechnology*, 2012, **23**, 444013.
15. L. Xu, L. Barcos and S. R. Nagel, *Physical Review E*, 2007, **76**, 066311.
16. A. Latka, A. Strandburg-Peshkin, M. M. Driscoll, C. S. Stevens and S. R. Nagel, *Physical review letters*, 2012, **109**, 054501.
17. G. Riboux and J. M. Gordillo, *Physical review letters*, 2014, **113**, 024507.
18. K. Yokoi, *Soft Matter*, 2011, **7**, 5120-5123.
19. C. Duetz, C. Ybert, C. Clanet and L. Bocquet, *Nat Phys*, 2007, **3**, 180-183.

20. L. Xu, W. W. Zhang and S. R. Nagel, *Physical review letters*, 2005, **94**, 184505.
21. P. Tsai, M. H. W. Hendrix, R. R. M. Dijkstra, L. Shui and D. Lohse, *Soft Matter*, 2011, **7**, 11325-11333.
22. S. D. Aziz and S. Chandra, *International journal of heat and mass transfer*, 2000, **43**, 2841-2857.
23. C. W. Visser, Y. Tagawa, C. Sun and D. Lohse, *Soft Matter*, 2012, **8**, 10732-10737.
24. M. H. W. Hendrix, R. Manica, E. Klaseboer, D. Y. C. Chan and C.-D. Ohl, *Physical review letters*, 2012, **108**, 247803.
25. J. C. Bird, R. Dhiman, H.-M. Kwon and K. K. Varanasi, *Nature*, 2013, **503**, 385-388.
26. V. Bergeron, D. Bonn, J. Y. Martin and L. Vovelle, *Nature*, 2000, **405**, 772-775.
27. C. Unger, J. Koch, L. Overmeyer and B. N. Chichkov, *Opt. Express*, 2012, **20**, 24864-24872.
28. S.-C. Tseng, C.-C. Yu, D.-C. Lin, Y.-C. Tseng, H.-L. Chen, Y.-C. Chen, S.-Y. Chou and L. A. Wang, *Nanoscale*, 2013, **5**, 2421-2428.
29. C. M. Rouleau, A. A. Puretzky and D. B. Geohegan, *Applied Physics Letters*, 2014, **105**, 213108.
30. S. Patankar, *Numerical heat transfer and fluid flow*, CRC Press, 1980.
31. P. Tsai, R. C. A. van der Veen, M. van de Raa and D. Lohse, *Langmuir*, 2010, **26**, 16090-16095.
32. S. Mandre and M. P. Brenner, *Journal of Fluid Mechanics*, 2012, **690**, 148-172.
33. C. W. Visser, P. E. Frommhold, S. Wildeman, R. Mettin, D. Lohse and C. Sun, *Soft Matter*, 2015, **11**, 1708-1722.
34. S. Sugden, *J. Chem. Soc., Trans.*, 1924, **125**, 32-41.



Journal Name

ARTICLE

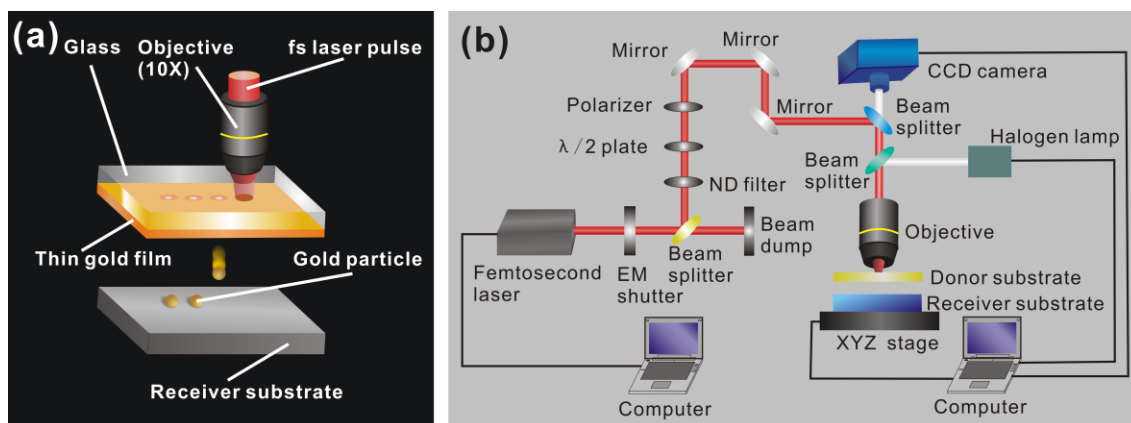


Fig. 1 (a) Schematic of the femtosecond laser induced forward transfer (fsLIFT) system for the generation of single submicron gold droplets. A thin gold film coating on glass is irradiated by a femtosecond laser pulse focused by the objective lens. A single submicron gold droplet is ejected from the film and impacts on a solid receiver substrate. (b) Schematic of the experimental setup used to study the impact of submicron gold droplets on a solid surface. The laser pulse is obtained from an electro-mechanical (EM) shutter. The pulse energy is varied using a neutral density (ND) filter, $\lambda/2$ plate and polarizer filter.

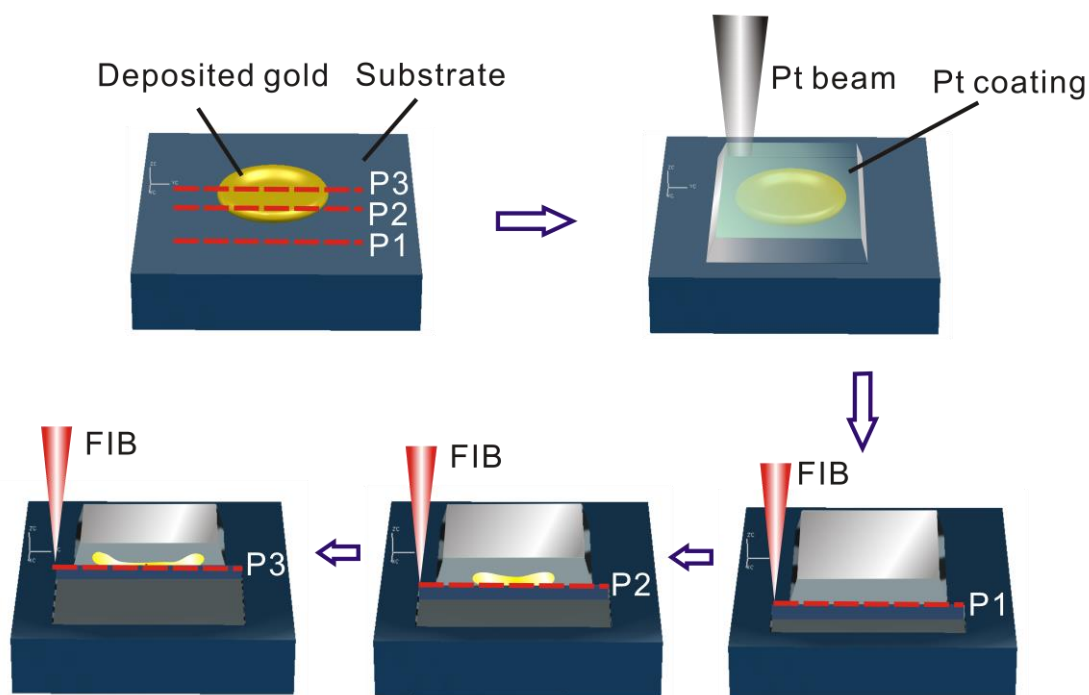


Fig. 2 Procedure involved in cross sectioning of the gold metal deposit on a substrate. A platinum coating is first deposited on the transferred gold deposit. This is followed by FIB milling proceeding vertically to the surface of the substrate from plane P1 and then to the central plane P3 in the gold deposit.

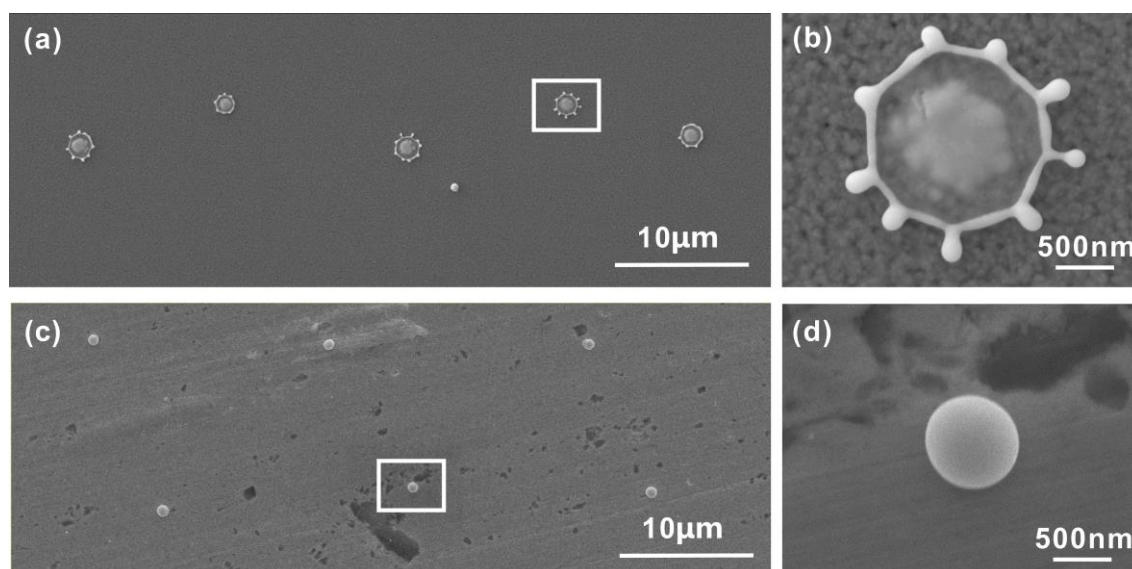


Fig. 3 Top view of transferred gold droplets after impact and splashing on the substrate. The droplets have an initial diameter of ~ 800 nm. (a) An array of gold droplets on the surface of a 50 nm gold film coating on silicon and with a molten gold droplet flight distance of $60 \mu\text{m}$. (b) Enlarged view of the transferred gold particle marked in Fig. 3a. (c) An array of gold droplets on the surface of a polished gold foil with a molten gold droplet flight distance of $120 \mu\text{m}$. (d) Enlarged view of the transferred gold particle marked in Fig. 3c.

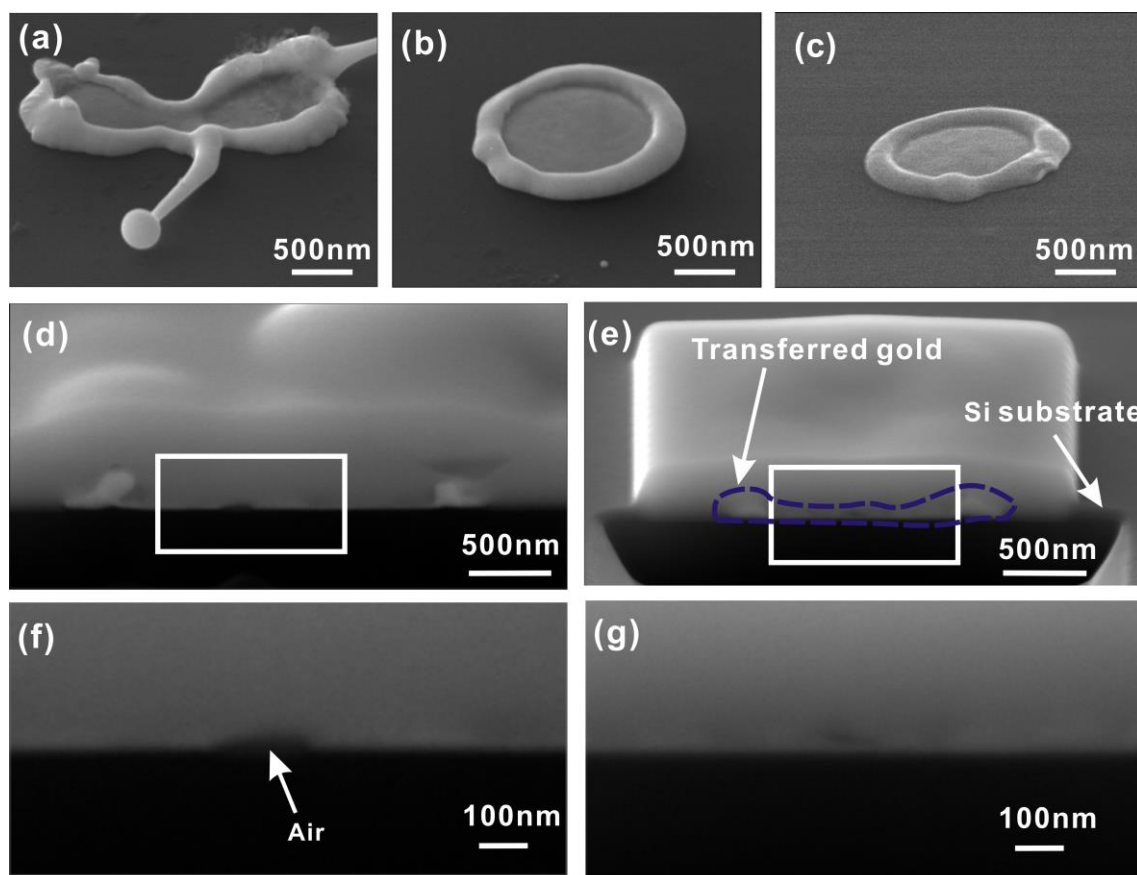


Fig. 4 Images of gold droplets (~ 800 nm in diameter) after impact on a silicon substrate surface. The flight distances are: (a) $<10 \mu\text{m}$, (b) $60 \mu\text{m}$, (c) $120 \mu\text{m}$. (d) and (e) are cross-sectional images of the transferred gold deposits shown in Fig. 4a and Fig. 4b respectively. (f) and (g) are magnified views of the areas on the cross-sections marked in Fig. 4d and Fig. 4e respectively. All images are taken at an angle of 55° , with the exception of that Fig. 4c which is taken at 45° .

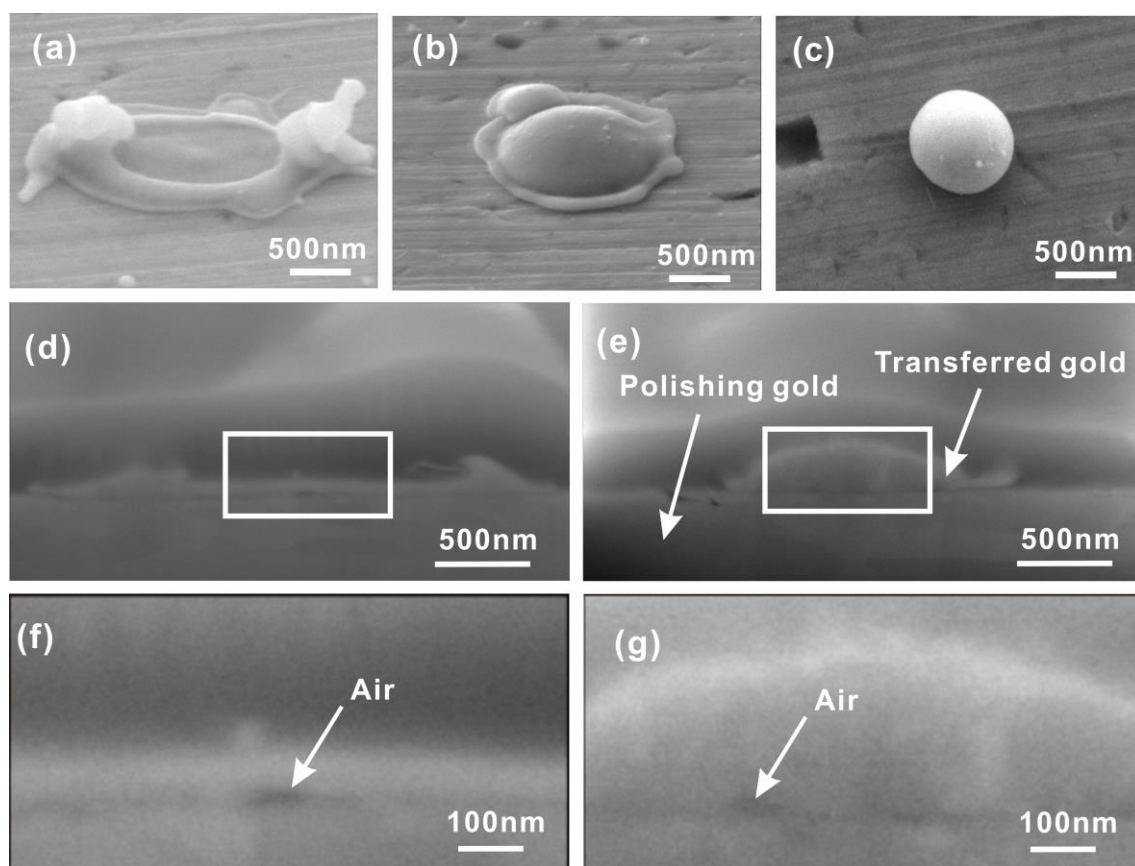


Fig. 5 Images of gold droplets (diameter ~ 800 nm) after impact on a polished gold foil surface. The flight distances are: (a) <10 μm , (b) 60 μm , (c) 120 μm . (d) and (e) are the cross-sectional images of the transferred gold deposits in Fig. 5a and Fig. 5b, respectively. (f) and (g) are magnified views of the areas in the cross-sections marked in Fig. 5d and Fig. 5e, respectively. All images are taken at an angle of 55° .

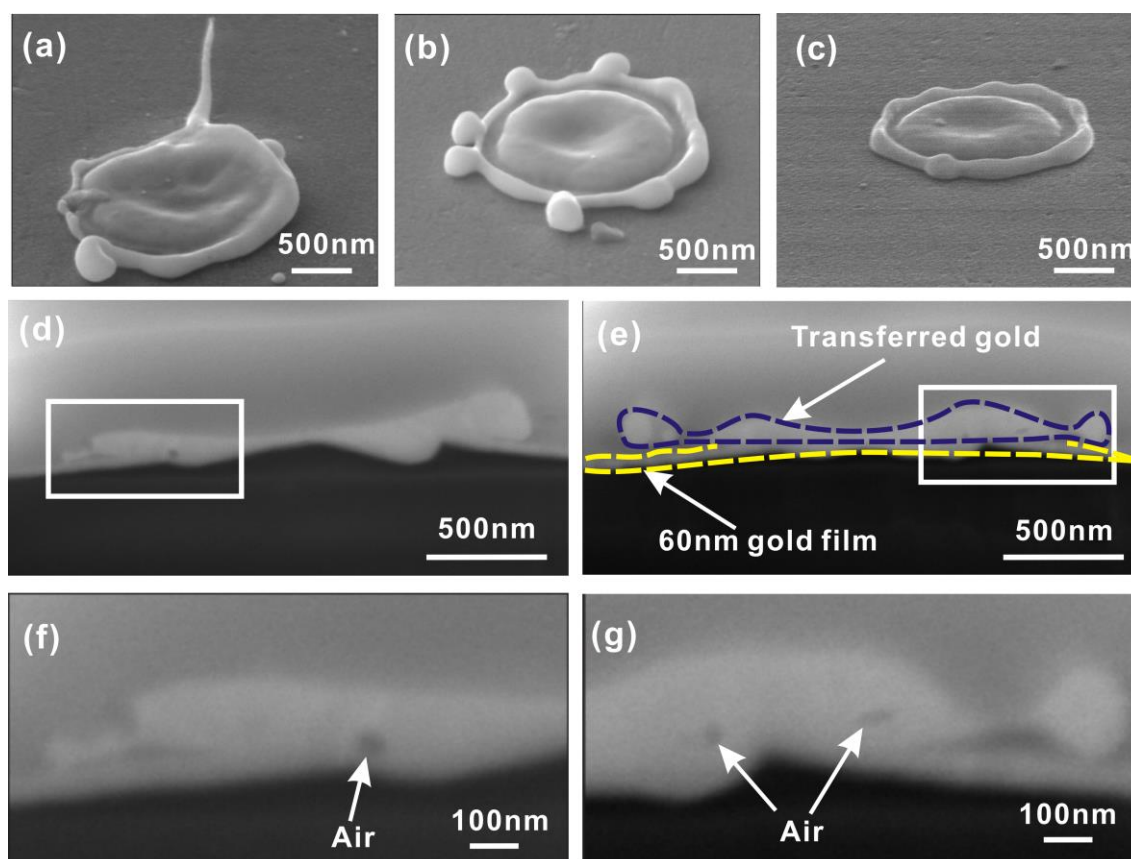


Fig. 6 Images of gold droplets (diameter ~ 800 nm) after impact on a 60 nm thick gold surface coating on glass. The flight distance are: (a) $<10\ \mu\text{m}$, (b) $\sim 60\ \mu\text{m}$, (c) $\sim 120\ \mu\text{m}$. (d) and (e) are the cross-sectional images of the transferred gold deposits in Fig. 6a and Fig. 6b respectively. (f) and (g) are magnified views of the areas in the cross-sections marked in Fig. 6d and Fig. 6e, respectively. All images are taken at an angle of 55° except that Fig. 5c which is taken at 45° .

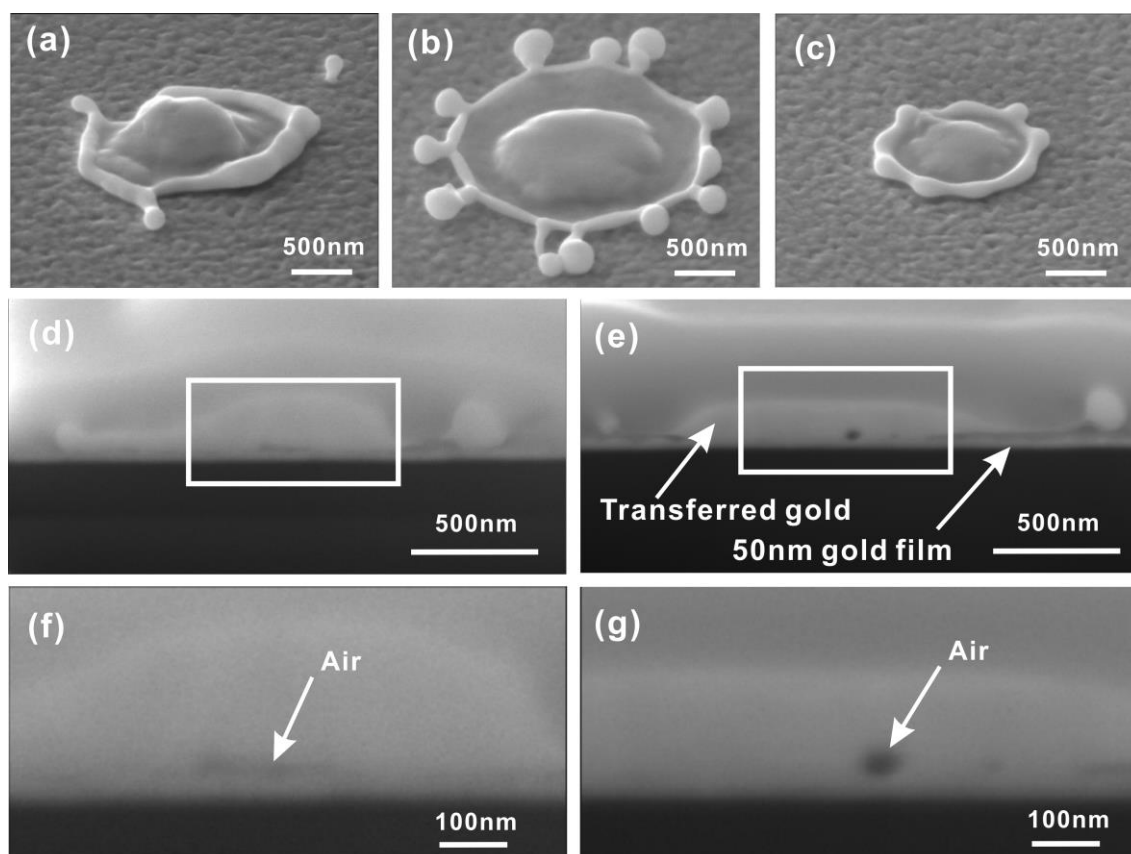


Fig. 7 Images of gold droplets (diameter ~ 800 nm) after impact on a 50 nm thick gold surface coating on silicon. The flight distances are: (a) $<10\ \mu\text{m}$, (b) $60\ \mu\text{m}$, (c) $120\ \mu\text{m}$. (d) and (e) are the cross-sectional images of the transferred gold deposits in Fig. 7a and Fig. 7b, respectively. (f) and (g) are magnified views of the cross-section marked in Fig. 7d and Fig. 7e respectively. All images are taken at an angle of 55° .

Table 1 Summary of splashing behaviors of sub-micron gold droplet impact on different substrates with different flight distances

Substrate	Average surface roughness (nm)	Droplet flight distance (μm)	Splashing or not ^a
Silicon	0.4	<10	▼
		~ 60	●
		~ 120	●
Polished gold foil	6.0	<10	▼
		~ 60	●
		~ 120	●
Gold coated glass	1.2	<10	▼
		~ 60	▼
		~ 120	●
Gold coated silicon	4.1	<10	▼
		~ 60	▼
		~ 120	●

^a observational results of SEM in describing whether sub-micron gold droplets splashed or not on that particular condition. Triangles mean splashing observed and circles mean no splashing observed.

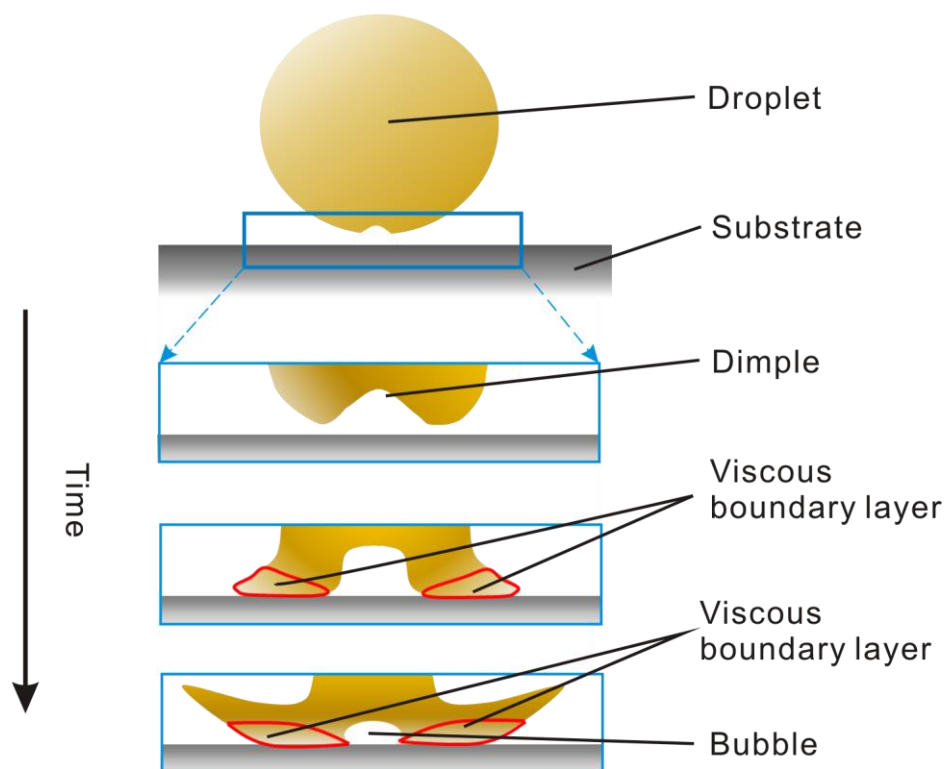


Fig. 8 Schematic showing of the different dynamic stages during droplet impact. The rectangular area in the top image is magnified in the subsequent images showing a cross-section of the droplet. Initially the droplet approaches close to substrate and forms a dimple due to compression of the ambient gas between the droplet and the surface. After contacting the substrate, viscous drag arising from the no-slip condition in the contact region causes the liquid in a boundary layer to rapidly decelerate. The liquid behind this region is then diverted upwards and forced to flow away from the surface. This conserves volume and initiates the ejection of metal in a splash morphology. This is accompanied by the formation of a bubble due to entraining of the air under the dimple.

A feasible technique was used to investigate splashing of molten sub-micron gold droplet: heat transfer was believed the key factor.

